Geophysical Prospecting, 2002, **50**, 183–194

Effective velocities in fractured media: a numerical study using the rotated staggered finite-difference grid

Erik H. Saenger* and Serge A. Shapiro

Freie Universität Berlin, Fachbereich Geophysik, Malteserstr. 74–100, Haus D, 12249 Berlin, Germany

Received December 2000, revision accepted July 2001

ABSTRACT

The modelling of elastic waves in fractured media with an explicit finite-difference scheme causes instability problems on a staggered grid when the medium possesses high-contrast discontinuities (strong heterogeneities). For the present study we apply the rotated staggered grid. Using this modified grid it is possible to simulate the propagation of elastic waves in a 2D or 3D medium containing cracks, pores or free surfaces without hard-coded boundary conditions. Therefore it allows an efficient and precise numerical study of effective velocities in fractured structures. We model the propagation of plane waves through a set of different, randomly cracked media. In these numerical experiments we vary the wavelength of the plane waves, the crack porosity and the crack density. The synthetic results are compared with several static theories that predict the effective P- and S-wave velocities in fractured materials in the long wavelength limit. For randomly distributed and randomly orientated, rectilinear, non-intersecting, thin, dry cracks, the numerical simulations of velocities of P-, SV- and SH-waves are in excellent agreement with the results of the modified (or differential) self-consistent theory. On the other hand for intersecting cracks, the critical crack-density (porosity) concept must be taken into account. To describe the wave velocities in media with intersecting cracks, we propose introducing the critical crack-density concept into the modified self-consistent theory. Numerical simulations show that this new formulation predicts effective elastic properties accurately for such a case.

1 INTRODUCTION

The prediction of effective elastic properties of fractured solids is of considerable interest for geophysics, material science and solid mechanics. In particular, it is important for constitutive modelling of brittle microcracking materials. For obvious practical reasons, the problem of a three-dimensional medium permeated by circular or elliptical planar cracks has received more attention in the literature. In this paper, we consider a fractured medium in two dimensions. This may seem to be a significant oversimplification. However, we believe that some broad generalizations can be elucidated that will help to solve problems with more complicated geometries.

Strong scattering caused by many dry or fluid-filled cracks can be treated only by numerical techniques because analytical solutions of the wave equation are not available. Boundary integral methods are well suited to handle such discrete scatterers in a homogeneous embedding. They allow the study of SH-waves (Davis and Knopoff 1995; Murai, Kawahara and Yamashita 1995), SV-waves (Dahm and Becker 1998) and P-waves (Kelner, Bouchon and Coutant 1999) in multiply fractured media, but they are currently restricted to non-intersecting cracks.

Finite-difference (FD) methods discretize the wave equation on a grid. They replace spatial derivatives with FD

*E-mail: saenger@geophysik.fu-berlin.de

operators using neighbouring points. The wavefield is also discretized in time; the wavefield for the next time-step is generally calculated using a Taylor expansion. Since the FD approach is based on the wave equation without physical approximations, the method accounts not only for direct waves, primary reflected waves and multiply reflected waves, but also for surface waves, head waves, converted reflected waves and waves observed in ray-theoretical shadow zones (Kelly *et al.* 1976). Additionally, it automatically accounts for the proper relative amplitudes. The paper of Andrews and Ben-Zion (1997) shows that, with respect to the accuracy, FD methods are at least as good as the boundary integral methods. Consequently, FD solutions of the wave equation are widely used to study scattering of waves by heterogeneities (e.g. Frankel and Clayton 1986; Kneib and Kerner 1993; Kusnandi *et al.* 2000).

The main idea behind using a staggered FD grid (Virieux 1986) is to calculate spatial derivatives half-way between two gridpoints to improve numerical accuracy. Hence, some modelling parameters are defined on inter-grid locations, in such a way that either they have to be averaged or the grid values half-way between two gridpoints have to be used. This can yield inaccurate results or instability problems when the propagation of waves in media with strong fluctuations of the elastic parameters (e.g. empty cracks) is simulated, even though the von Neumann stability criterion (see e.g. Crase 1990) is fulfilled. In the present numerical study, however, we apply the rotated staggered grid (Saenger, Gold and Shapiro 2000) for the modelling of elastic wave propagation in arbitrary heterogeneous media. The rotated staggered grid is briefly discussed in Section 3.1.

We present a numerical study of effective velocities of two types of fractured 2D medium. We model the propagation of a plane wave through a well-defined fractured region. The numerical set-up is described in Section 3.2. We use randomly distributed and randomly orientated, rectilinear, dry, thin cracks in both media. For the first type of medium, we examine only non-intersecting cracks. The numerical results for P-, SV- and SH-waves (see Section 3.3) are compared comprehensively with several theories (see Section 2.2) that predict the effective velocities for such a case. Additionally, we compare our results with the numerical results of Davis and Knopoff (1995), Murai *et al.* (1995) and Dahm and Becker (1998). The second type of fractured medium contains intersecting cracks. For this case the theories for non-intersecting cracks and boundary integral methods are beyond their range of validity. However, we have found that the theory of Mukerji *et al.* (1995), including a so-called critical-porosity concept, can be applied to take into account intersecting cracks. By combining the concept of critical porosity (i.e. critical crack density) with the so-called modified self-consistent theory, we propose in Section 2.3 a new analytical formulation that is able to handle the case of intersecting cracks. The predictions of this new heuristic formalism are in excellent agreement with our numerical results shown in Section 3.4.

2 THEORY

2.1 Formulae for transversely isotropic media

All our 2D fractured media models are filled at random with randomly orientated, rectilinear, dry, thin cracks (i.e. crack locations as well as crack orientations are random). Therefore, we consider 2D statistically isotropic media. In 3D space our models are homogeneous along the spatial direction that is perpendicular to the plane of our 2D models. Therefore, from a theoretical point of view, our fractured 2D models also represent a 3D, transversely isotropic, fractured situation with symmetry axis perpendicular to the 2D plane.

To describe the wave propagation in anisotropic media we use the same notation as Thomsen (1986). The elastic moduli and the velocities are related by the well-known formulae:

$$\rho_g v_{SV}^2(90^o) = c_{44}, \tag{1}$$

$$\rho_g v_{SH}^2(90^o) = c_{66}, \tag{2}$$

$$\rho_g v_P^2(90^o) = c_{11}, \tag{3}$$

where c_{11}, c_{44} and c_{66} are elements of the stiffness tensor, ρ_g is the gravitational density, and $v_{SV}(90^o)$, $v_{SH}(90^o)$ and $v_P(90^o)$ are the phase velocities of SV-, SH- and P-waves propagating perpendicular to the symmetry axis of the transversely isotropic medium.

2.2 Non-intersecting cracks

In this section we consider randomly distributed and randomly orientated, rectilinear, non-intersecting, thin, dry cracks in 2D media (Fig. 1). Papers by Kachanov (1992) and Davis and Knopoff (1995) provide sound descriptions of theoretical approaches in this case. Both papers discuss three different theories for 2D media that predict an effective velocity for fractured models, namely, the 'theory for non-interacting cracks' (NIC), the 'self-consistent theory' (SC) and the 'modified (or differential) self-consistent theory' (MSC). They can be used to predict effective wave velocities

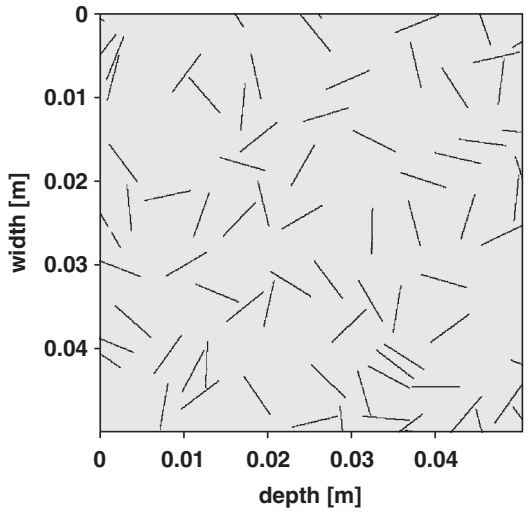

Figure 1 Randomly distributed and randomly orientated, rectilinear, *non-intersecting*, thin, dry cracks in homogeneous 2D media. A part of model No. 7.1 is shown (see Table 1).

in the long wavelength limit. In order to compare later our numerical results with different theoretical predictions, we summarize here the ideas and results for these theories. For the definition of the crack-density parameter ρ (Kachanov 1992), we use

$$\rho = \frac{1}{A}\sum_{k=1}^{n} l_k^2, \tag{4}$$

where $2l_k$ is the length of rectilinear cracks, n is the number of cracks and A is the representative area.

First, we concentrate on one type of shear wave: SH(90°)-waves. The theory for non-interacting cracks (NIC) is derived for the case of a dilute crack density. It assumes that the energy per unit crack length needed for inserting a single anti-plane crack is simply added n times to the energy of the unfractured medium. With this assumption, the effective shear modulus $< \mu_{\rm NIC} >$ ($\hat{=} < c_{66} >$) (Davis and Knopoff 1995) can be calculated:

$$< \mu_{\rm NIC} > = \mu_0 \frac{1}{1 + \pi(\rho/2)}, \tag{5}$$

where μ_0 is the shear modulus of the unfractured isotropic medium and ρ is the crack density.

In the simplest form of self-consistent (SC) calculations, to determine the properties at higher orders, it is argued that an individual crack is introduced into an already cracked medium and hence should be subjected to the stress field in the flawed system (i.e. in the effective medium) and not to that in the unflawed system (O'Connell and Budiansky 1974, 1976; Budiansky and O'Connell 1976). This yields the following prediction for the effective shear modulus $< \mu_{\rm SC} >$:

$$< \mu_{\rm SC} > = \mu_0[1 - \pi(\rho/2)]. \tag{6}$$

However, Chatterjee, Mal and Knopoff (1978), Hudson (1980) and Hudson and Knopoff (1989) showed that although the interaction between cracks is considered in the self-consistent model, the dipole–dipole interactions are neglected and may have a practical importance at high crack densities.

Two other studies (Bruner 1976; Henyey and Pomphrey 1982) argue that the change in energy should be calculated sequentially by introducing new cracks in sequentially alternated effective media. This argument leads to the shear modulus as the solution to a simple differential equation. The result of such a consideration, called the modified (or differential) self-consistent (MSC) theory, is the following exponential formula for the effective shear modulus $< \mu_{\rm MSC} >$:

$$< \mu_{\rm MSC} > = \mu_0 {\rm e}^{-\pi(\rho/2)}. \tag{7}$$

To complete our overview we state the formulae for effective moduli (plane strain case) from the three theories for P(90°)- and SV(90°)-waves (Kachanov 1992; Yuan 1998):

$$\begin{bmatrix} < c_{11} > & < c_{12} > & 0 \\ < c_{12} > & < c_{11} > & 0 \\ 0 & 0 & < c_{44} > \end{bmatrix} = \begin{bmatrix} \frac{1-\upsilon_0^2}{<E>} & -\frac{\upsilon_0(1+\upsilon_0)}{E_0} & 0 \\ -\frac{\upsilon_0(1+\upsilon_0)}{E_0} & \frac{1-\upsilon_0^2}{<E>} & 0 \\ 0 & 0 & \frac{1}{<G>} \end{bmatrix}^{-1}. \tag{8}$$

- Theory for non-interacting cracks:

$$< E_{\rm NIC} > = E_0 \frac{1}{1 + \pi\rho}, \tag{9}$$

$$< G_{\rm NIC} > = G_0 \frac{1}{1 + \pi(1 - \upsilon_0)\rho}. \tag{10}$$

- Self-consistent theory:

$$< E_{\rm SC} > = E_0(1 - \pi\rho), \tag{11}$$

$$< G_{\rm SC} > = G_0(1 - \pi(1 - \upsilon_0)\rho). \tag{12}$$

- Modified (differential) self-consistent theory:

$$< E_{\rm MSC} > = E_0 {\rm e}^{-\pi\rho}, \tag{13}$$

$$< G_{\rm MSC} > = G_0 {\rm e}^{-\pi(1 - \upsilon_0)\rho}. \tag{14}$$

In these equations, E_0 denotes Young's modulus, G_0 denotes shear modulus (controlling propagation of SV-waves in this symmetry) and υ_0 is Poisson's ratio of the unfractured

isotropic medium. Note that to the first order (i.e. including terms up to $\mathbf{O}(\pi\rho)$), all three theories predict the same effective moduli. Figure 5 illustrates the theories for non-intersecting cracks (for $v_0 = 0.25$).

2.3 Intersecting cracks

Let us now consider randomly distributed and randomly orientated, rectilinear, intersecting, thin, dry cracks in 2D media (Fig. 2). The theories described in Section 2.2 are not applicable in this case, because they are derived specifically for non-intersecting cracks. For example, for a crack density of $\rho = 1.43$, the effective modulus predicted by the modified self-consistent theory for SH(90°)-waves (equation (7)) is $< \mu > = 0.10\ \mu_0$. But at this crack density in the case of intersecting cracks, a modulus of $< \mu > = 0$ can be observed because there is no path for the wave through the skeleton of the fractured medium. In the case of intersecting cracks the medium clearly demonstrates a kind of percolation behaviour. It is a monolith for small ρ. However, it falls apart for large ρ. Therefore, to predict the effective velocities it is necessary to use another approach that takes into account such critical behaviour.

In the case of porous media, Mukerji *et al.* (1995) proposed the differential effective medium (DEM) theory (Norris 1985; Zimmermann 1991) modified by including the concept of the critical porosity (Nur 1992). Note that in this formalism the effective velocities are predicted in terms of porosity ϕ rather than in terms of crack density ρ.

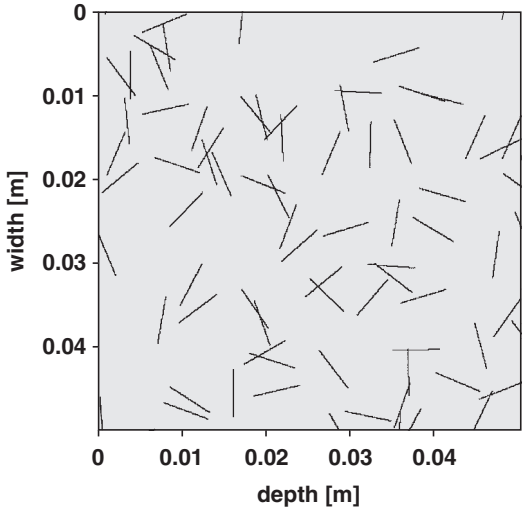

Figure 2 Randomly distributed and randomly orientated, rectilinear, *intersecting*, thin, dry cracks in homogeneous 2D media. A part of model No. 10x.1 is shown (see Table 1).

The first step in using this modified DEM theory for fractured media is to determine the critical porosity (or the critical crack density). At the percolation porosity, the material is a loose packing of grains barely touching each other. This value of the percolation (i.e. critical porosity) can be derived with the help of percolation theory (see e.g. Sahimi 1995). The special case of percolation in fractured 2D models is discussed and calculated by Robinson (1983, 1984). The result corresponding to our models (intersecting, rectilinear, random, thin cracks of constant length in 2D media) is a critical crack density of $\rho_c = 1.43$ (or a critical porosity of $\phi_c = 0.13$). For $\rho > \rho_c$, only finite-size pieces of the solid exist, and there is no continuum through which an elastic wave can propagate. This is illustrated in Fig. 1 of Robinson (1983).

The second step is to calculate the effective elastic parameters at the critical porosity. The moduli at the percolation point are equal to the Reuss (harmonic) average (Mavko, Mukerji and Dvorkin 1998) of the constituent moduli, because in the general case of filled pores or cracks the medium tends to a suspension. In our case of dry cracks we obtain (by calculating the Reuss average) a value of zero for all elastic moduli at the critical density. This is a clear consequence of the absence of the propagation continuum.

The third step is to calculate the effective moduli with respect to the porosity. For arbitrarily distributed cracks in 3D we have to solve two coupled differential equations (Berryman 1992) with critical-porosity initial conditions that can be found in Mukerji *et al.* (1995). Using this approach we observed that the predicted effective velocity for S-waves for needle-like inclusions (Eshelby 1957; Wu 1966; Berryman 1980) is in good agreement with numerical results for SH (90°)-waves in 2D media with intersecting cracks (Saenger and Shapiro 2000).

However, our 2D fractured models with rectilinear cracks represent 3D transversely isotropic media with symmetry axis perpendicular to the 2D plane. The modified DEM theory is (so far) derived only for 3D isotropic fractured media. 3D transversely isotropic fractured media have been discussed for dilute crack densities, for example by Nur (1971). The difficulty of incorporating percolation behaviour in a DEM theory is the requirement of a solution for high crack densities. Some general ideas in this direction can be found in Cheng (1993).

On the other hand, the physical concepts of the DEM and MSC theories have a lot in common. The most important here is the principle of sequential introduction of new cracks leading in simple situations to exponential formulae

for effective moduli. Taking this into account we suggest a new heuristic critical crack density (CCD) formulation for 2D (i.e. 3D transversely isotropic) fracturing configurations. We introduce into the results of the MSC theory (described in Section 2.2) an additional factor to include the physical behaviour at the critical crack density. We propose the following formulae (compare with (7), (13) and (14)):

$$< \mu_{\mathrm{CCD}} > = \mu_0 \mathrm{e}^{-\pi(\rho/2)\left(\frac{\rho_\mathrm{c}}{\rho_\mathrm{c}-\rho}\right)^n}, \tag{15}$$

$$< E_{\mathrm{CCD}} > = E_0 \mathrm{e}^{-\pi\rho\left(\frac{\rho_\mathrm{c}}{\rho_\mathrm{c}-\rho}\right)^n}, \tag{16}$$

$$< G_{\mathrm{CCD}} > = G_0 \mathrm{e}^{-\pi(1-\nu_0)\rho\left(\frac{\rho_\mathrm{c}}{\rho_\mathrm{c}-\rho}\right)^n}, \tag{17}$$

where ρ_c denotes the critical crack density.

This heuristic formalism fulfils the following important conditions:

- For the critical crack density the elastic moduli are zero. For example:

$$\lim_{\rho\to\rho_\mathrm{c}} < \mu_{\mathrm{CCD}} > = 0. \tag{18}$$

- For an infinite critical crack density the theory gives the same predictions as the MSC theory. The necessity of this limit follows from the physically evident fact that an infinite critical crack density for randomly distributed and orientated, rectilinear, thin cracks implies non-intersecting cracks. For example:

$$\lim_{\rho_\mathrm{c}\to\infty} < \mu_{\mathrm{CCD}} > = < \mu_{\mathrm{MSC}} > . \tag{19}$$

- For dilute crack densities the CCD formulation gives (to first order) the same predictions as the MSC theory. For example:

$$\frac{\partial}{\partial\rho} < \mu_{\mathrm{CCD}} > (0) = \frac{\partial}{\partial\rho} < \mu > (0), \tag{20}$$

$$< \mu_{\mathrm{CCD}} > (0) = < \mu_{\mathrm{MSC}} > (0) = < \mu_0 > . \tag{21}$$

The effective velocities of SH(90°)-, SV(90°)- and P(90°)-waves predicted by this new CCD formulation are plotted in Fig. 7 with solid lines ($\upsilon_0 = 0.25$, $\rho_\mathrm{c} = 1.43$, $n = 0.5$).

3 NUMERICAL EXPERIMENTS

3.1 Finite-difference modelling of fractured media

The propagation of elastic waves is described by the elastodynamic wave equation (e.g. Aki and Richards 1980),

$$\rho_\mathrm{g}(\mathbf{r})\ddot{u}_i(\mathbf{r}) = \left(c_{ijkl}(\mathbf{r})\mathbf{u}_{k,l}(\mathbf{r})\right)_{,j} + f_i(\mathbf{r}). \tag{22}$$

For modelling elastic waves at the position i with finite differences, it is necessary to discretize the stiffness tensor c_{ijkl}, the gravitational density ρ_g, the displacement wavefield u_i and the body force f_i on a grid.

3.1.1 *The standard staggered grid*

A standard method of discretizing staggered grids (Kneib and Kerner 1993) is shown in Fig. 3(a). The main reason for using this method is to improve numerical accuracy with respect to centred FD grids. There is only one density location and one location for the Lamé parameter μ in this elementary cell. Thus the calculation of the stress component σ_{xz} has to be carried out by multiplying the values of strain and stiffness defined at different positions. This leads to the necessity of replacing, for example, the density at the left and the lower side by the density of the centre and replacing the shear modulus at the lower left corner by the shear modulus at the centre. The same difficulties arise for the calculation of the acceleration, since the density must be taken from a different location. When the wavefield hits inhomogeneities (e.g. cracks) with high contrasts of elastic parameters or density, stability problems can occur. Here we obtain an unstable modelling of a wavefield diffraction on a crack (Saenger *et al.* 2000). Note that such stability problems exist even though the von Neumann stability criterion (e.g. Crase 1990) is fulfilled.

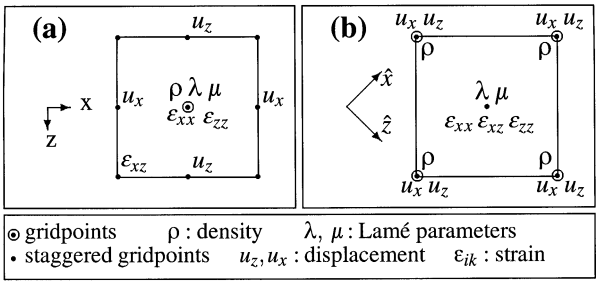

Figure 3 Elementary cells showing locations where strains, displacement and elastic parameters are defined. (a) Locations are shown on a standard staggered grid if no averaging of medium parameters is performed. (b) Elementary cell of the rotated staggered grid. Spatial derivatives are performed along the $\hat{x}$- and $\hat{z}$-axes. The wave equation and the elements of the stiffness tensor are the same as in (a).

3.1.2 The rotated staggered grid

All the difficulties described above can be avoided by choosing another configuration of the grid (Saenger *et al.* 2000). By placing all components of the strain tensor at the same position within the elementary grid cell (e.g. the centre), the positions of the modelling parameters (i.e. displacements) and of the medium parameters are found directly as shown in Fig. 3(b). The directions of spatial derivatives have rotated from $\mathbf{x}$ and $\mathbf{z}$ to $\hat{\mathbf{x}}$ and $\hat{\mathbf{z}}$.

The grid in Fig. 3(b) satisfies all stability and positioning conditions with respect to the operations that are necessary to perform a time-step. The parameters that have to be multiplied are defined at the same location and derivatives are defined between the locations of parameters that have to be differentiated. Since the density is not located at the same position as the stiffness tensor elements, two alternatives are possible. The density can be given on an additional (staggered) grid. Another, more practical approach suggests a density averaging using the four surrounding cells. In the case of homogeneous cells or a linear behaviour of the density between the stiffness locations, the density coincides with the exact density after averaging. The new distribution of elastic parameters is also advantageous for modelling in general anisotropic media, because no interpolation is necessary to calculate the Hook sum in the modelling algorithm (Igel, Mora and Riollet 1995).

Note that the FD approach used by Andrews and Ben-Zion (1997), in contrast to the rotated staggered grid, is based on a triangular elementary cell. However, the distribution of modelling parameters in such a grid is, in principle, similar to those in the rotated staggered grid technique and, therefore, can also be applied when modelling high-contrast elastic media.

3.1.3 Stability and dispersion

Frequency-dependent velocity errors, also called numerical dispersion, cannot be excluded completely but can be estimated and, therefore, reduced to a known and acceptable degree. The dispersion errors for the rotated staggered grid are similar to those of the conventional staggered grid (Saenger *et al.* 2000).

As previously stated, the von Neumann stability criterion is not used in connection with the stability problems for high-contrast inclusions. For the rotated grid the von Neumann stability criteria for the 3D and 2D cases are the same. We obtain

$$\frac{\Delta t v_{\mathrm{P}}}{\Delta h} \leq 1 \Big/ \left(\sum_{k=1}^{n} |c_k| \right), \tag{23}$$

where c_k denotes the difference coefficients (e.g. central limit coefficients (Karrenbach 1995)), v_{P} the compressional wave velocity, Δt the time increment and Δh the grid spacing. This result yields the von Neumann stability criterion for the rotated staggered grid at all wave numbers in the case of a homogeneous medium, and a second-order operator in time.

For a more detailed description of the rotated staggered grid refer to Saenger *et al.* (2000).

3.2 Experimental set-up

The rotated staggered FD scheme is a powerful tool for testing theories about fractured media. The formalisms discussed in Section 2 predict the effective elastic moduli of multiply fractured media as a function of crack density ρ or porosity ϕ. In order to test the formalisms we designed some numerical elastic models which include a region with a well-known crack density and porosity.

The cracked region was filled at random with randomly orientated cracks. For models with non-intersecting cracks the same procedure as in Davis and Knopoff (1995) and Dahm and Becker (1998) is used: if two cracks intersected during random selection, the more recent crack was eliminated and a random choice was made again. Figure 4(a) shows a typical model with non-intersecting cracks. This model contains 1000×1910 gridpoints with an interval of 0.0001 m. In the homogeneous region we set $v_{\mathrm{P}} = 5100$ m/s, $v_{\mathrm{S}} = 2944$ m/s and $\rho_{\mathrm{g}} = 2700$ kg/m^3. Table 1 summarizes the relevant parameters for all the models we use in our experiments. For the dry cracks we set $v_{\mathrm{P}} = 0$ m/s, $v_{\mathrm{S}} = 0$ m/s and $\rho_{\mathrm{g}} = 0.0001$ kg/m^3, which approximates a vacuum. Thus each additional crack increases the porosity.

We perform our modelling experiments with periodic boundary conditions in the horizontal direction. For this reason our elastic models are also generated with this periodicity. Hence, it is possible for a single crack to start at the right side of the model and to end at its left side.

To obtain effective velocities in different models we apply a body force line source at the top of the model. The plane wave generated in this way propagates in a downward direction through the fractured medium (see Fig. 4).

With two horizontal lines of 1000 receivers at the top (depth = 0.01 m) and at the bottom (depth = 0.152 m), it is possible to measure the time-delay of the mean peak

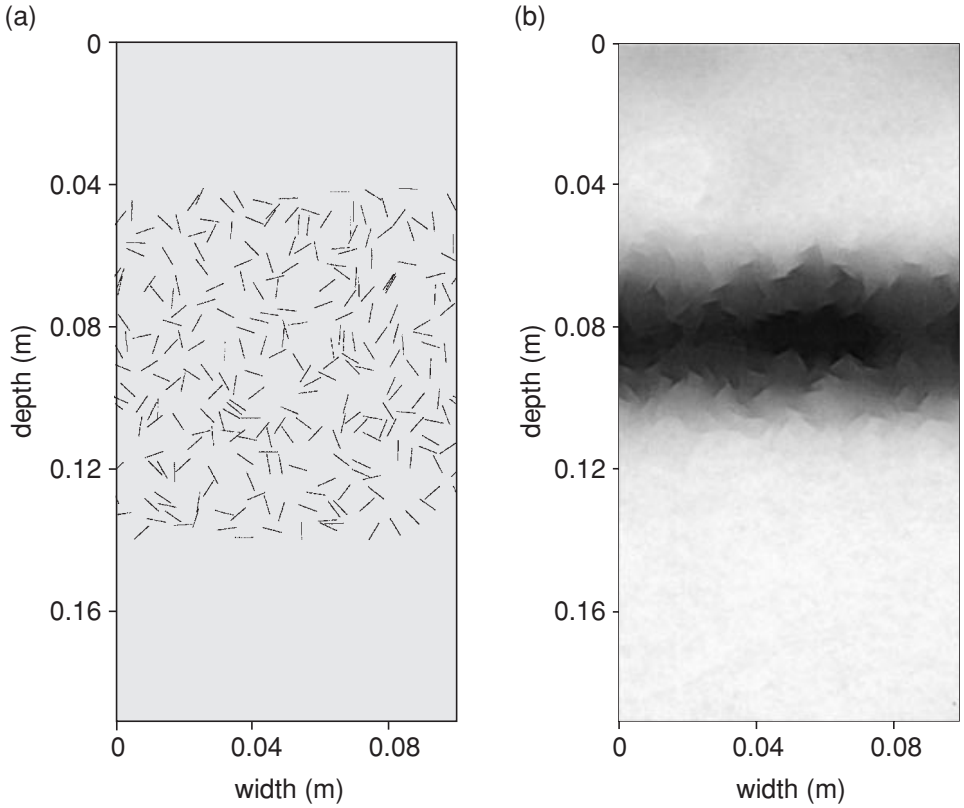

Figure 4 (a) A typical fractured model (No. 7.1 of Table 1) used for the numerical experiments. We introduce a cracked region into a homogeneous material. At the top we place a small vacuum strip. This is advantageous for applying a body force line source with the rotated staggered grid. (b) A snapshot of an SH-plane wave propagating through the cracked region (black indicates high amplitude).

Table 1 Crack models for numerical calculations. The models denoted with an x have intersecting cracks. The width of the cracks is equal to the grid spacing. NB 0.0001 m is the size of the grid spacing and the size of the crack region is always 1000×1000 gridpoints

No.	Crack density ρ	Length of cracks [0.0001 m]\ aspect ratio of cracks	Number of cracks	Porosity ϕ of the crack region	Number of model realizations
1.1–1.4	0.200	7 \ 0.14	15280	0.1407	4
2.1–2.7	0.200	14 \ 0.077	3881	0.0708	7
3	0.200	28 \ 0.04	996	0.0358	1
4	0.025	56 \ 0.021	31	0.0022	1
5	0.050	56 \ 0.021	63	0.0046	1
6.1–6.6	0.100	56 \ 0.021	126	0.0091	6
7.1–7.11	0.200	56 \ 0.021	252	0.0181	11
8.1–8.7	0.300	56 \ 0.021	378	0.0360	7
9x	0.050	56 \ 0.021	63	0.0045	1
10x	0.100	56 \ 0.021	126	0.0091	1
11x.1–11x.6	0.200	56 \ 0.021	252	0.0181	6
12x	0.300	56 \ 0.021	378	0.0270	1
13x.1–13x.6	0.401	56 \ 0.021	504	0.0360	6
14x	0.601	56 \ 0.021	756	0.0539	1
15x	0.801	56 \ 0.021	1007	0.0720	1

amplitude of the plane wave caused by the inhomogeneous region. The effective velocity can be estimated from this time-delay. Additionally, the attenuation of the plane wave can be studied. Note that the time-delay and the attenuation do not depend significantly on the particular realization of our model for a given fixed crack density. This will be demonstrated in the following with error bars.

The direction of the body force and the source wavelet (i.e. source time function) can vary to generate two types of shear (SH- and SV-) wave and one longitudinal (P-) wave. The source wavelet in our experiments is always the first derivative of a Gaussian, with different dominant frequencies, and with a time increment $\Delta t = 5 \times 10^{-9}$ s. Table 2 gives details of the wavelets.

All computations are performed with second-order spatial FD operators and with a second-order time update. In order to reduce the dispersion error we use only 25% of the allowed maximum time increment ($\gamma = 0.25\gamma_{\max}$; see Saenger *et al.* 2000). The number of gridpoints per dominant wavelength N_λ depends on the wavelet used in the modelling, and is in general larger than 588 (see Table 2). Therefore, with this configuration our measurements are, for a model with a crack density of $\rho = 0$, velocities of $v_P = 5101.86$ m/s (relative error: 0.036%) and $v_S = 2943.62$ m/s (relative error: 0.013%). To obtain such accurate modelling results with up to 40 000 time-steps we have to use large-scale parallel computers (e.g. Cray T3E). Owing to this computational cost we have to restrict ourselves to significant cases of model variations in determining the error bars.

The number of gridpoints per dominant wavelength N_λ is also important when modelling small-scale structures. Saenger *et al.* (2000) show an accurate modelling of a single arbitrarily shaped crack with $N_\lambda \geq 14$. It is generally known that increasing N_λ improves the numerical accuracy for arbitrarily steep structures (e.g. Robertsson 1996).

Table 2 Parameters of the different wavelets used in the numerical study. NB 0.0001 m is the size of the grid spacing

No.	f_{dom} (Hz)	P-wavelength (dom.) [0.0001 m]	S-wavelength (dom.) [0.0001 m]
1	2200000	23	13
2	800000	64	37
3	400000	128	74
4	120000	425	245
5	50000	1020	588
6	22000	2318	1338

3.3 Numerical results for non-intersecting cracks

The numerical results on effective wave velocities for non-intersecting cracks are depicted by dots in Fig. 5. For comparison, the predictions of the three theories described above are also shown.

We show the normalized effective velocities for three types of wave. The relative decrease in the effective velocity for a given crack density is smallest for SH-waves, followed by SV-waves, and is largest for P-waves. For each wave type, we perform numerical FD calculations with five different crack densities. For the case of non-intersecting cracks we use model Nos 4, 5, 6.1–6.5, 7.1–7.11, 8.1–8.7 ($2l = 0.0056m$, Table 1) and the wavelet No. 5 ($\lambda_{\text{dom}}(\text{S}) = 0.0588$ m, $\lambda_{\text{dom}}(\text{P}) = 0.1020$ m, Table 2). The ratio of the crack length to the dominant wavelength is given by the parameter p,

$$p = \frac{2l}{\lambda_{\text{dom}}} \tag{24}$$

(rectilinear cracks of length $2l$, dominant wavelength λ_{dom}). Hence these calculations give a value of $p = 0.095$ for S-waves, and $p = 0.055$ for P-waves. As Murai *et al.* (1995) conclude, this is a very good approximation to reach the long wavelength limit.

The aspect ratio of the cracks we used in our numerical experiments should not influence significantly the results of the three theories for non-intersecting cracks discussed (compare with Douma 1988). It is important to note that, for a dilute crack density (e.g. $\rho = 0.025$), the numerical results and all three theories match very well. This is an additional analytical argument for the accuracy of our numerical study. A final result is that our numerical simulations of P-, SV- and SH-wave velocities are in excellent agreement with the predictions of the modified (or differential) self-consistent theory.

Next we examine the influence of the ratio of crack length to the dominant wavelength on our results. The ratio is given by p (equation (24)). We restrict ourselves to studying only the influence of this ratio using one single crack density ($\rho = 0.2$) and for SH-waves with vibration direction perpendicular to the 2D model. This enables us to compare our results with the results of Davis and Knopoff (1995) because they use the same mode of deformation and randomly distributed and randomly orientated cracks. In contrast to our study, Murai *et al.* (1995) considered a fractured situation with randomly distributed parallel cracks and a crack density of $\rho \leq 0.02$.

There are two possibilities of varying the parameter p. The first possibility is to vary λ_{dom} by using all the wavelets in

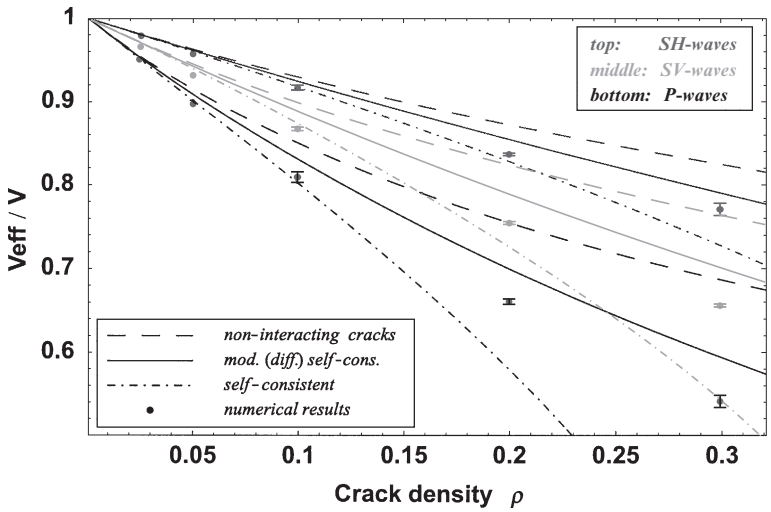

Figure 5 Normalized effective velocity versus crack density. Dots: numerical results of this study. The error bar denotes the standard deviation for different model realizations (see Table 1). The three dashed lines are predicted by the theory for non-interacting cracks, the three dashed–dotted lines by the self-consistent theory and the three solid lines by the modified (or differential) self-consistent theory. The top curves result from SH(90°)-waves. The other shear-wave results (SV(90°)-waves) are depicted in the middle. The bottom curves result from compressional P(90°)-waves. Details are given in Sections 2.2 (theory) and 3.3 (numerical results).

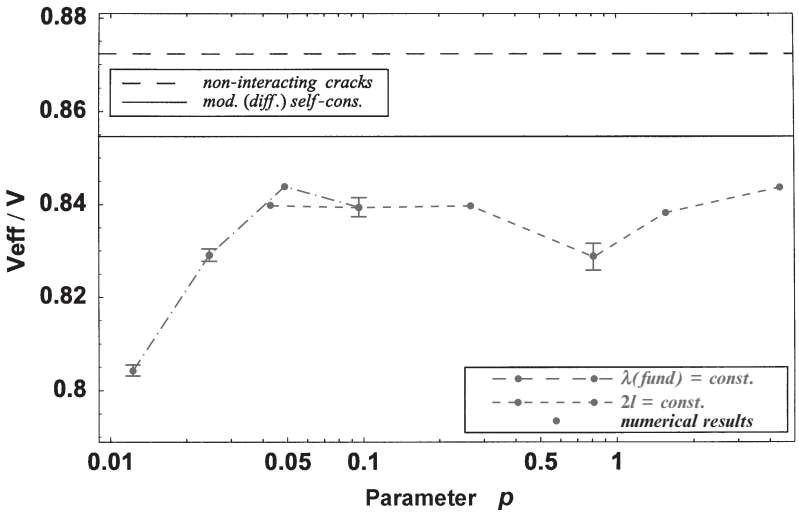

Figure 6 Normalized effective velocity (SH-waves) versus $p = 2l/\lambda_{\mathrm{dom}}$ (normalized frequency), for crack density $\rho = 0.2$. Dots: numerical results of this study. Two horizontal lines at the top: different theoretical predictions. The error bar denotes the standard deviation for different model realizations (see Table 1). Note that the numerical result shown at $p = 0.095$ is also shown in Fig. 5. Details are given in Section 3.3.

Table 2 and not to change the length of the cracks using model No. 7 (Table 1). The numerical results are shown in Fig. 6 (dots joined with dashed line). The three theories for non-intersecting cracks mentioned above are derived for wavelengths much larger than the crack length (discussed e. g. by Peacock and Hudson 1990). Therefore, it is interesting to observe that over a wide range of p (by varying λ_{dom}) there is no significant change in the effective velocity.

For the second curve in Fig. 6 (dots joined with dashed-dotted line), we always use wavelet No. 5 and vary the length of the cracks using model Nos 1.1–1.4, 2.1–2.7, 3, 7.1–7.11 (see Table 2). Note that with decreasing length of cracks the porosity of the fractured region increases. Hence, the decrease in the effective velocity for small values of p on this curve can be explained by the increasing influence of the porosity of the models used.

An additional result is that our calculated effective velocities (dots in Fig. 6) always match the prediction by the modified self-consistent theory (solid horizontal line) better than the prediction by the theory for non-interacting cracks (dashed horizontal line) for all values of p. This fact underlines the numerically based conclusion that the modified self-consistent theory always predicts effective velocities most accurately.

This is in contrast to some conclusions by Davis and Knopoff (1995). They proposed that the theory for non-interacting cracks is valid for much higher crack densities than expected. Dahm and Becker (1998) conducted a similar

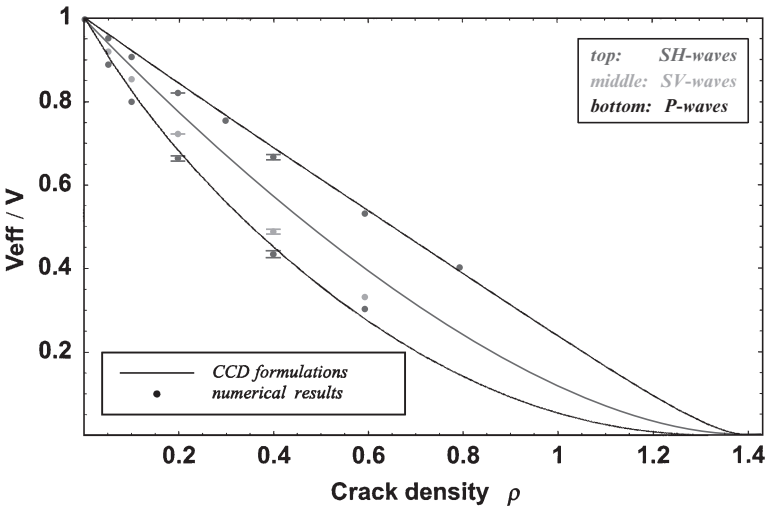

Figure 7 Normalized effective SH-, SV- and P-wave velocities for intersecting cracks versus crack density. Dots: numerical results of this study. Lines: theoretical predictions of the CCD formulations. The error bar denotes the standard deviation for different model realizations (see Table 1). Details are given in Sections 2.3 (theory) and 3.4 (numerical results).

boundary integral experiment and an additional finite-element study, and found that crack–crack interactions cannot simply be ignored for high crack densities. The findings of these two papers have been further discussed by Liu, Hudson and Pointer (2000) and Le Ravalec and Guéguen (1996). The conclusions of Dahm and Becker (1998) are in agreement with our results. Even the fact that the numerically calculated effective velocities tend to be slightly lower than the effective velocities predicted by the MSC theory is consistent with our numerical simulations. A detailed discussion about why this discrepancy can arise in different studies can be found in Dahm and Becker (1998).

3.4 Numerical results for intersecting cracks

Our numerical results for intersecting cracks are shown in Fig. 7. For the calculations of normalized effective velocities marked with dots we always use wavelet No. 5 (Table 2) and model Nos 9x, 10x, 11x.1–11x.6, 12x, 13x.1–13x.6, 14x, 15x (Table 1).

We show the calculations for all three wave types. The relative decrease of the effective velocity for a given porosity is smallest for SH-waves followed by SV-waves, and is largest for P-waves.

Our numerical results and the new CCD formulation, including a critical crack density, are in excellent agreement. It is important to note that the value of $n = 0.5$, used to determine the effective velocities predicted by (15)–(17) in Fig. 7, is fixed empirically (best fit).

4 CONCLUSIONS

We have presented a numerical tool, a rotated staggered FD grid, to calculate effective velocities in fractured media. Finite-difference modelling of the elastodynamic wave equation is very fast and accurate. In contrast to a standard staggered grid, high-contrast inclusions do not cause instability difficulties for our rotated staggered grid. Thus, our numerical modelling of elastic properties of dry-rock skeletons can be considered as an efficient and well-controlled computer experiment.

We considered 2D isotropic (3D transversely isotropic) fractured media. We have numerically tested predictions of three different theoretical approaches: the theory for non-interacting cracks, the self-consistent theory and the modified self-consistent theory. For non-intersecting, rectilinear, thin, dry cracks, the modified (differential) self-consistent (MSC) theory is most successful in predicting effective velocities for SV-, SH- and P-waves.

For the case of intersecting fractures it is important to take percolation behaviour of the medium into account. The concept of the critical crack density may be introduced to explain the elastic properties of such media. We propose a heuristic approach termed the critical crack density (CCD) formulation. This combines the critical crack-density concept with the modified (differential) self-consistent media theory. The CCD formulation predicts effective velocities for SV-, SH- and P-waves in fractured 2D media with intersecting, rectilinear, thin, dry cracks. The numerical results support predictions of this new empirical formulation.

ACKNOWLEDGEMENTS

We thank the German Research Society (DFG; Sonderforschungsbereich 267 and 381) and the Wave Inversion Technology (WIT) Consortium-project for their financial support. We thank M. Karrenbach for providing us with his parallel FD program for further modifications. We are grateful to E.A. Robinson, P. Hubral and L.W.B. Leite for helpful discussions and suggestions. We also thank Associate Editor E. Liu, T. Pointer, and one anonymous reviewer for their thoughtful comments and suggestions. The simulations were performed at the HLR Stuttgart (Project 11172).

REFERENCES

Aki K. and Richards P.G. 1980. *Quantitative Seismology: Theory and Methods*. W.H. Freeman & Co.

Andrews D.J. and Ben-Zion Y. 1997. Wrinkle-like slip pulse on a fault between different materials. *Journal of Geophysical Research* **102**, 553–571.

Berryman J.G. 1980. Long-wavelength propagation in composite elastic media; i. spherical inclusions and ii. ellipsoidal inclusions. *Journal of the Acoustical Society of America* **68**, 1809–1831.

Berryman J.G. 1992. Single-scattering approximations for coefficients in Biot's equations of poroelasticity. *Journal of the Acoustical Society of America* **91**, 551–571.

Bruner W.M. 1976. Comment on "Seismic velocities in dry and saturated cracked solids" by R.J. O'Connell and B. Budiansky. *Journal of Geophysical Research* **81**, 2573–2576.

Budiansky B. and O'Connell R.J. 1976. Elastic moduli of a cracked solid. *International Journal of Solids and Structures* **12**, 81–97.

Chatterjee A., Mal A. and Knopoff L. 1978. Elastic moduli of a cracked solid. *Journal of Geophysical Research* **83**, 1785–1792.

Cheng C.H. 1993. Crack models for a transversely isotropic medium. *Journal of Geophysical Research* **98**, 675–684.

Crase E. 1990. High-order (space and time) finite-difference modelling of the elastic wave equation. 60th SEG meeting, San Francisco, USA, Expanded Abstracts, 987–991.

Dahm T. and Becker T. 1998. On the elastic and viscous properties of media containing strongly interacting in-plane cracks. *Pure and Applied Geophysics* **151**, 1–16.

Davis P.M. and Knopoff L. 1995. The elastic modulus of media containing strongly interacting antiplane cracks. *Journal of Geophysical Research* **100**, 18253–18258.

Douma J. 1988. The effect of the aspect ratio on crack-induced anisotropy. *Geophysical Prospecting* **36**, 614–632.

Eshelby J.D. 1957. The determination of the elastic field of an ellipsoidal inclusion, and related problems. *Proceedings of the Physical Society of London, A* **241**, 376–396.

Frankel A. and Clayton R.W. 1986. Finite difference simulations of seismic scattering: implications for the propagation of short-period seismic waves in the crust and models of crustal heterogeneity. *Journal of Geophysical Research* **91**, 6465–6489.

Henyey F.S. and Pomphrey N. 1982. Self-consistent elastic moduli of a cracked solid. *Geophysical Research Letters* **9**, 903–906.

Hudson J. 1980. Elastic moduli of a cracked solid. *Mathematical Proceedings of the Cambridge Philosophical Society* **88**, 371–384.

Hudson J. and Knopoff L. 1989. Predicting the overall properties of composites – material with small-seale inclusions or cracks. *Pure and Applied Geophsics* **131**, 551–576.

Igel H., Mora P. and Riollet B. 1995. Anisotropic wave propagation through finite-difference grids. *Geophysics* **60**, 1203–1216.

Kachanov M. 1992. Effective elastic properties of cracked solids: critical review of some basic concepts. *Applied Mechanics Review* **45**, 304–335.

Karrenbach M. 1995. *Elastic tensor wavefields*. PhD thesis, Stanford University.

Kelly K.R., Ward R.W., Treitel S. and Alford R.M. 1976. Synthetic seismograms: a finite-difference approach. *Geophysics* **41**, 2–27.

Kelner S., Bouchon M. and Coutant O. 1999. Numerical simulation of the propagation of P waves in fractured media. *Geophysical Journal International* **137**, 197–206.

Kneib G. and Kerner C. 1993. Accurate and efficient seismic modelling in random media. *Geophysics* **58**, 576–588.

Kusnandi, van Baren G., Mulder W., Herman G. and van Antwerpen V. 2000. Sub-grid finite-difference modelling of wave propagation and diffusion in cracked media. 70th SEG meeting, Calgary, Canada, Expanded Abstracts, ST P1.2.

Le Ravalec M. and Guéguen Y. 1996. Comment on "The elastic modulus of media containing strongly interacting antiplane cracks" by Paul M. Davis and Leon Knopoff. *Journal of Geophysical Research* **101**, 25373–25375.

Liu E., Hudson J.A. and Pointer T. 2000. Equivalent medium representation of fractured rock. *Journal of Geophysical Research* **105**, 2981–3000.

Mavko G., Mukerji T. and Dvorkin J. 1998. *The Rock Physics Handbook*. Cambridge University Press.

Mukerji T., Berryman J., Mavko G. and Berge P. 1995. Differential effective medium modelling of rock elastic moduli with critica porosity constraints. *Geophysical Research Letters* **22**, 555–558.

Murai Y., Kawahara J. and Yamashita T. 1995. Multiple scattering of SH waves in 2D elastic media with distributed cracks. *Geophysical Journal International* **122**, 925–937.

Norris A.N. 1985. A differential scheme for the effective moduli of composites. *Mechanics of Materials* **4**, 1–16.

Nur A. 1971. Effects of stress on velocity anisotropy in rocks with cracks. *Journal of Geophysical Research* **76**, 2022–2034.

Nur A. 1992. Critical porosity and the seismic velocities in rocks (abstract). *EOS Transactions AGU* **73**, 66.

O'Connell R.J. and Budiansky B. 1974. Seismic velocities in dry and saturated cracked solids. *Journal of Geophysical Research* **79**, 5412–5426.

O'Connell R.J. and Budiansky B. 1976. Reply. *Journal of Geophysical Research* **81**, 2577–2578.

Peacock S. and Hudson J.A. 1990. Seismic properties of rocks with distributions of small cracks. *Geophysical Journal International* **102**, 471–484.

Robertsson J.O.A. 1996. A numerical free-surface condition for elastic/viscoelastic finite-difference modelling in the presence of topography. *Geophysics* **61**, 1921–1934.

Robinson P.C. 1983. Connectivity of fracture systems – a percolation theory approach. *Journal of Physics A: Math. Gen.* **16**, 605–614.

Robinson P.C. 1984. Numerical calculations of critical densities for lines and planes. *Journal of Physics A: Math. Gen.* **17**, 2823–2830.

Saenger E.H., Gold N. and Shapiro S.A. 2000. Modelling the propagation of elastic waves using a modified finite-difference grid. *Wave Motion* **31**, 77–92.

Saenger E.H. and Shapiro S.A. 2000. Calculation of effective velocities in fractured media using the rotated staggered grid. 62nd EAGE conference, Glasgow, UK, Extended Abstracts, D-34.

Sahimi M. 1995. *Flow and Transport in Porous Media and Fractured Rock*. VCH, Weinheim, Germany.

Thomsen L. 1986. Weak elastic anisotropy. *Geophysics* **51**, 1954–1966.

Virieux J. 1986. Velocity-stress finite-difference method. *Geophysics* **51**, 889–901.

Wu T.T. 1966. The effect of inclusion shape on the elastic moduli of a two-phase material. *International Journal of Solids and Structures* **2**, 1–8.

Yuan F.G. 1998. *Lecture on Anisotropic Elasticity*. Mars Mission Research Center, Department of Mechanical and Aerospace Engineering, North Carolina State University, Raleigh, NC 27695.

Zimmermann R.W. 1991. *Compressibility of Sandstones*. Elsevier Science Publishing Co.